Quasiplanarity of the Peptide Bond

Jakub Chalupský, Jiří Vondrášek,* and Vladimír Špirko*

Center for Biomolecules and Complex Molecular Systems, Institute of Organic Chemistry and Biochemistry, Academy of Sciences of the Czech Republic, v.v.i., Flemingovo nám.2, 160 10 Prague 6, Czech Republic

Received: June 29, 2007; In Final Form: October 18, 2007

The vibrational motions of the model peptide unit represented by the main-chain carbonyl carbon, oxygen, nitrogen, and amide hydrogen are analyzed quantum-mechanically using formamide, *cis-N*-methylformamide, *trans-N*-methylformamide, *N,N*-dimethylformamide, L-alanyl-L-alanine, and *N*-benzoylphenylalanine as dynamical models. To make this analysis computationally feasible, the peptide unit vibrational motions were first separated from the remaining molecular vibrational motions by means of the crude adiabatic (Born−Oppenheimer) approximation, and then, using the same approximate separation, the peptide unit dynamical problem was separated into sets of high- and low-frequency subproblems. Importantly, the simplest dynamical (one-dimensional) problem based on the separation of the amide out-of-plane motion from the rest of the peptide unit motions allows for a physically correct description of the effective "ground state" molecular geometry of all studied systems. The separation is thus believed to be also suitable for reliable estimation of the dynamical effects on the geometry of the peptide unit in other molecular systems.

Introduction

The peptide unit according to the IUPAC-IUB definition including the group of atoms −CHR−C═O−NH− is an essential structural element of proteins. Due to conjugation between the carbonyl and amine groups (see Figures 1 and 2), the CN bond (known as a peptide bond) has a partial double-bond character, which prevents internal rotation around this bond. Consequently, the whole arrangement of the four C, O, N, H atoms and two attached carbon atoms is expected to be planar. The peptide bond and its planarity are among the essential structural features discovered by Pauling[1,2] and successfully applied to properties of secondary structure elements. On the other hand, Ramachandran showed that nonplanarity of peptide bonds is an internal property of cyclic peptides; thus there is need for nonplanarity as another feature in polypeptide chains.[3] According to numerous theoretical and experimental studies (see, e.g., refs 4−13), however, the peptide unit atoms exhibit a quasiplanar arrangement with departures from planarity, which should be considered in any quantitative refining of X-ray and NMR structures and rationalizing of NMR relaxation data (see, e.g., refs 14−16). Esposito[4] confirmed that significant departure from planarity is strictly correlated with the values of the adjacent ψ angle, e.g., that the side chain character on the C_α adjacent to the carbonyl carbon influences the peptide bond properties. Therefore, to complete these studies, accurate dynamical calculations are necessary. The only practical way to perform such calculations while taking all relevant dynamical degrees of freedom into consideration is to utilize molecular dynamics simulations (see, e.g., ref 8 and references therein), which are feasible even in the case of very large systems and ideally suited for the exploration of structural dynamical effects. However, the accuracy of these calculations is strongly limited by the drawbacks of the available representations of molecular force fields. In the case of the peptide unit, these representations seem to fail especially in describing the pyramidalization phenomena at the peptide unit nitrogen atom.[7,8,17] As in the case of the amino unit of the nucleic acid bases,[18] pyramidalization of the peptide unit is a truly collective motion (involving all the unit atoms), which is opposed by a profoundly anharmonic potential (see, e.g., ref 7). Consequently, using the standard normal coordinate based vibrational models for describing its dynamics (see, e.g. ref 8 and references therein) is inadequate; more suitable alternatives are desirable. One such alternative has already been probed by Brown et al.,[19] where these authors, using the so-called semirigid-bender vibrational Hamiltonian,[20] reanalyzed all the vibration−rotation data of formamide related to the molecular planarity and its out-of-plane NH_2 vibration. The analysis has revealed that (a) formamide possesses a very shallow single-minimum inversion potential, (b) during inversion, the amino group rotates around the CN bond with the *syn*-hydrogen staying closer to the NCO plane than the *anti*-hydrogen, (c) the formyl

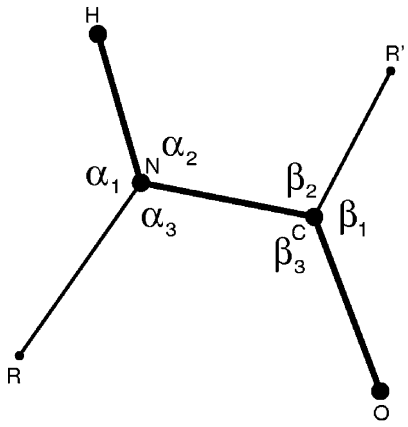

Figure 1. Definition of internal coordinates in the peptide unit.

* Corresponding authors. E-mail: J.V., vondrasek@marge.uochb.cas.cz; V.S., spirko@marge.uochb.cas.cz.

10.1021/jp0750699 CCC: $40.75
Published on Web 01/05/2008

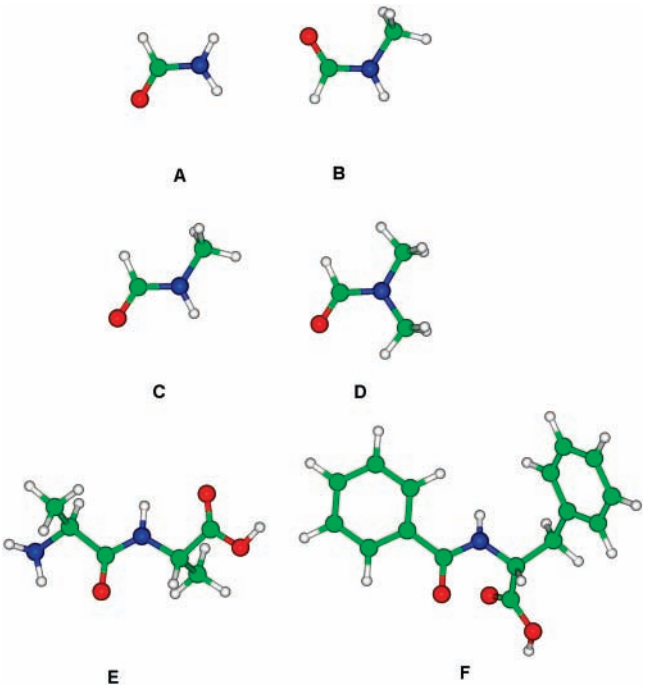

Figure 2. CPK ball and stick models of studied molecules: (A) formamide; (B) *N*-methylformamide (*trans*); (C) *N*-methylformamide (*cis*); (D) *N*,*N*-dimethylformamide; (E) L-alanyl-L-alanine; (F) *N*-benzoylphenylalanine.

hydrogen moves in the direction opposite to that of the amino hydrogens, whereas the CN bond lengthens as the amino hydrogens move out-of-plane. Similar findings were also obtained for cyanamide and vinylamine[21,22] and are promising in terms of the transferability of the forces associated with pyramidalization motion.

Although formally one-dimensional, the semirigid-bender approach allows for all the important interaction terms from potential energy as well as rotation−vibration interaction terms from kinetic energy, namely by making it possible for the molecular valence coordinates to vary with the reference coordinate (i.e., the inversion coordinate in the case of formamide and vinylamine). The shapes of these variations are *a priori* unknown, and their determination requires the corroboration of appropriate experimental or *ab initio* data.

The semirigid-bender approach is formally simple and easily extensible to larger molecular systems. However, the approach is also beset by inaccuracy, which cannot be determined within its framework. Therefore, to gain insight into its prospects and reliability in the case of larger peptides/proteins, we found it worthwhile to probe it within the framework of the nonrigid-bender approach,[23,24] which enables a quantitative accounting for the dynamical interactions. The actual probing is performed by means of model calculations using formamide, *cis*-*N*-methylformamide, *trans*-*N*-methylformamide, *N*,*N*-dimethylformamide, L-alanyl-L-alanine and *N*-benzoylphenylalanine as model molecules. The calculations are kept feasible by reducing the dimensionality of the dynamical problems by means of the adiabatic (Born−Oppenheimer) separation of motions with various energy contents (see, e.g., refs 25 and 26).

Computational Details

The *ab initio* calculations are performed stepwise. In the first step, the equilibrium geometry (energy global minimum) and vibrationally distorted geometries (energy optima for molecular configurations described by fixed values of explicitly treated vibrational coordinates with the remaining geometry parameters allowed to relax) are determined by means of the Gaussian program suite.[27] For formamide, *cis*-*N*-methylformamide, *trans*-*N*-methylformamide, and *N*,*N*-dimethylformamide the MP2 method[28] is used with the AUG-cc-pVDZ basis set.[29] The structures of L-alanyl-L-alanine and *N*-benzoylphenylalanine were taken from the Cambridge structural database (CSD)[30] under the CSD identifiers ALALHC[31] and ECAMIE.[32] The optimization calculations on L-alanyl-L-alanine and *N*-benzoylphenylalanine are performed using the RI-MP2/AUG-cc-pVDZ approach[33] and the B3LYP functional[34] with the 6-31G** basis set,[35] respectively. In the second step, the actual (grid-point) energies of the equilibrium and vibrationally distorted molecular structures are calculated using the CCSD/AUG-cc-pVDZ approach[36] for formamides and the RI-MP2 and RI-CC2 (ref 37) approaches (as implemented in the Turbomole program[38] with the AUG-cc-pVDZ auxiliary "RI" basis set[39] for L-alanyl-L-alanine and *N*-benzoylphenylalanine, respectively.

The dynamical calculations are performed within the framework of the nonrigid-bender formalism[23,24] using a nonrigid molecular reference following closely the N out-of-plane (ρ) motion and geometrically defined (curvilinear) valence coordinates (Φ) measuring the vibrational displacements from this reference. The appropriate Hamiltonian acquires the following form

$$\mathbf{H} = \frac{1}{2}\mu_{\rho\rho}J_\rho^{\,2} + \frac{1}{2}\sum_{k,l\in\Phi} G_{kl}P_kP_l + V(\rho,\Phi) + V_{\text{pseudo}}(\rho,\Phi) \quad (1)$$

In (1), Φ is the vector of the vibrational coordinates; the quantum mechanical operators corresponding to J_ρ and P_m are $-i\hbar(\partial/\partial\rho)$ and $-i\hbar(\partial/\partial m)$, respectively; $V(\rho,\Phi)$ is the total potential energy; $V_{\text{pseudo}}(\rho,\Phi)$ comprises all the terms arising from the vibrational dependence of $\mu_{\rho\rho}$ (the out-of-plane component of the tensor, which is the inverse of the 4×4 generalized (HBJ) molecular inertia tensor) and G_{kl} (the matrix elements of the generalized vibrational **G** matrix); for details see refs 24 and 40.

Effective, state-dependent molecular geometries are evaluated as the following average valence bond lengths/angles

$$g_{val}^{i} = \langle\Psi_i(\rho,\Phi)|g_{val}(\rho,\Phi)|\Psi_i(\rho,\Phi)\rangle \quad (2)$$

where $\Psi_i(\rho,\Phi)$ is the vibrational wavefunction of a given vibrational state *i*.

To make a comparison for comparing with diffraction data involving contributions from all the populated molecular states possible, the following thermal average characteristics are also evaluated

$$\langle g_{\text{val}}\rangle_T = \Sigma_j g_{\text{val}}^{j} e^{-E_j/kT}/\Sigma_j e^{-E_j/kT} \quad (3)$$

where E_j are vibrational energies, T is a vibrational temperature, and k is the Boltzmann constant.

Results and Discussion

Formamide. The simplest molecular model for studying dynamical properties of the OCNH peptide unit is provided by the formamide molecule. Nevertheless, despite this simplicity (which is only relative as the molecule possesses 12 vibrational degrees of freedom), the abundance of highly accurate microwave and infrared spectral data,[41−48] and numerous theoretical

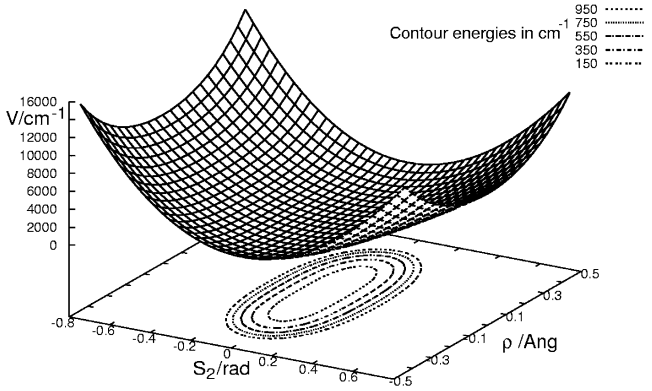

Figure 3. $V_{\rho,S_2,S_3=0}$ section of the total potential energy of formamide.

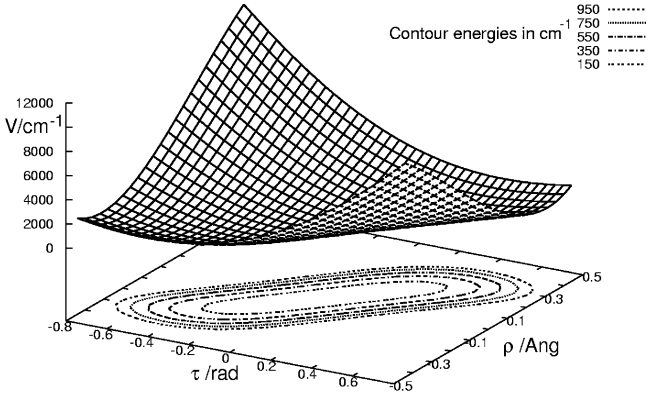

Figure 4. $V_{\rho,\tau}$ section of the total potential energy of formamide.

studies (see, e.g., refs 49 and 50 and references therein), resolving its structure may still seem to be a delicate problem: whereas the most accurate theoretical studies strongly support its planarity, the experimental data can be rationalized equally well by considering it to be either planar or nonplanar. In our opinion, the uncertainty concerning the molecular planarity is only apparent because of an improper comparison of the equilibrium theoretical characteristics with the experimental data, which were affected by the dynamical effects of molecular vibrations. To prove this, we ran several dynamical calculations and evaluated dynamically corrected characteristics, which are suitable for comparison with the available experimental data. To gain insight into the accuracy limits of the semirigid-bender model being probed, three kinds of dynamical calculations were performed using the following adiabatic separations for the total vibrational wavefunction $\Psi(\rho,\Phi)$

$$\Psi(\rho,\Phi) = \psi(\rho)\,\chi(\Phi;\rho) \tag{4}$$

$$\Psi(\rho,\Phi) = \psi(\rho,S_2,S_3)\,\chi(\Phi';\rho,S_2,S_3) \tag{5}$$

and

$$\Psi(\rho,\Phi) = \psi(r_{NH'},r_{NH''},r_{CN})\,\chi(\Phi'';r_{NH'},r_{NH''},r_{CN}) \tag{6}$$

where the out-of-plane coordinate ρ measures the distance of the N atom from the plane formed by the C atom and the H atoms of the NH_2 group; and the symmetry coordinates S_2 and S_3 are the following combinations of the valence angles of the CNH_2 fragment (see Figure 1)

$$S_2 = (2\alpha_1 - \alpha_2 - \alpha_3)/6^{1/2} \tag{7}$$

and

$$S_3 = (\alpha_2 - \alpha_3)/2^{1/2} \tag{8}$$

and, Φ, Φ', and Φ'', the "remaining" vibrational coordinates, are assumed to respond adiabatically to the changes in the explicitly treated motions ρ, S_2, S_3, and $r_{NH'}$, $r_{NH''}$, r_{CN}, respectively.

Obviously, the first separation scheme (4) provides the first-principles theoretical rationalization of the semirigid-bender theory for the ρ motion in a one-dimensional potential $V_{eff}(\rho)$, generated by the remaining molecular motions. In the second scheme (5), the pyramidalization at the N atom is treated as a collective bending motion in an effective energy-minimum-path potential $V_{eff}(\rho,S_2,S_3)$ obtained through optimizing molecular energies on a three-dimensional $\rho \otimes S_2 \otimes S_3$ grid of molecular configurations. The third type of the adiabatic separations (6) describes the N atom, which involves stretching ("high-frequency") motions adiabatically separated from the other molecular motions.

From the aspect of the energy contents of the vibrational degrees of freedom, fairly quantitative separation of the molecular motions can be expected for the low-frequency ($\nu_{ofp} \sim 300$ cm^{-1}) out-of-plane and high-frequency ($\nu_{NH} \sim 3500$ cm^{-1}) NH stretching motions. Less quantitative results are to be expected for the separation of the out-of-plane and medium-frequency ($\nu_{CN} \sim 1250$ cm^{-1}) CN stretching motions (the purpose of treating of the slower CN stretching motion simultaneously with the truly high-frequency NH stretchings in Scheme (6) is to account for the relatively strong "CN vs NH" kinematic interactions). The suitability of the adiabatic separation (4) of the out-of-plane motion from the vibrational bending motions involving the NH_2 fragment is shown in Figures 3 and 4 (the couplings of the S_3 bending and $OCNH_{cis}$ dihedral motions with the out-of-plane motion are the very same as those of their S_2 and $OCNH_{trans}$ counterparts): Although the energy minimum motion is opposed by a very shallow potential, the motions "perpendicular" to it are hindered by steeper potentials. From this point of view, the out-of-plane motion is the only low-frequency motion of formamide and may be thus assumed to be reasonably tractable by means of a one-dimensional theory (4). Apparently, a fairly accurate separation can be expected when dealing

TABLE 1: Experimental and Calculated Vibrational Frequencies of Formamide (in cm^{-1})

mode	exp[a]	exp[b]	calc 1[c]	calc 2[d]	calc 3[e]	calc 4[f]	calc 5[g]	calc 6[h]	calc 7[i]
$^{a}\nu_{NH}$	**3570**	3566	3958		3754	**3609**	3560		
$^{s}\nu_{NH}$	**3448**	3443	3825		3605	**3486**	3531		
ν_{CN}	**1255**	1260	1334		1281	**1309**	1320		
ν_{inv}	**288.7**		402.5	294.0	114.3	**285.8**	295 0	**283.0**	292.4
$2\nu_{inv}$	**657.3**		805.0	655.3	228.6	**650.0**	681.9	**648.4**	681.4
$3\nu_{inv}$	**1058.3**		1207.5	1049.2	342.9	**1059.1**	1122.9	**1064.4**	1124.4

[a] Reference 46. [b] Reference 47. [c] Calculated using the class II peptide quantum mechanical force field.[17] [d] Semirigid−bender calculations.[19] [e] This study: Harmonic approximation. [f] This study: 3D calculations ("exact" kinetic energy). [g] This study: 3D calculations (approximate kinetic energy). [h] This study: 1D calculations ("exact" kinetic energy). [i] This study: 1D calculations (approximate kinetic energy).

TABLE 2: Experimentally Determined and Calculated Molecular Geometries of Formamide[a]

source	r_{NH}^{trans}	r_{NH}^{cis}	r_{CN}	r_{CH}	r_{CO}	α_1	α_2	α_3	β_1	β_2	β_3	τ^{trans}	τ^{cis}
exp[b]	1.002(5)	1.014(5)	1.376(10)	1.102(10)	1.193(20)	118.88(67)	120.62(67)	117.15(67)	122.97(67)	113.14(67)	123.80(67)	12(5)	7(5)
exp[c]	1.002(3)	1.002(3)	1.352(12)	1.095(10)	1.219(12)	121.6(3)	120.0(5)	118.5(5)	122.5(20)	112.7(20)	122.5(20)	0.0	0.0
exp[d]	1.027	1.027	1.368	1.125	1.212	121.6	119.7	118.7	122.3	112.7	125.0	0.0	0.0
calc 1[e]	1.000	1.003	1.354	1.097	1.212	119.6	121.1	119.3	123.0	112.0	125.0	0.0	0.0
calc 2[f]	1.00986	1.01245	1.36793	1.11051	1.22832	119.63	121.11	119.26	122.83	112.60	124.57	0.0	0.0
calc 3[g]	1.01200	1.01501	1.37381	1.11039	1.22803	117.32	119.19	117.55	122.78	112.63	124.61	15.5	8.6
calc 4[h]	1.01138	1.01378	1.37192	1.11040	1.22803	118.04	119.59	117.86	122.79	112.52	124.65	16.0	8.0

[a] Bond distances in Å, valence angles in degrees. [b] Reference 43. Nonplanar structure assumed. [c] Reference 44. Planar r_s structure. [d] Reference 54. Planar structure assumed. [e] Best theoretical estimate of the equilibrium structure.[50] [f] This study: equilibrium structure. [g] This study, ground state: 3D calculations ("exact" kinetic energy). [g] This study, ground state: 1D calculations ("exact" kinetic energy).

TABLE 3: Inversional Molecular Geometries of Formamide[a]

state	r_{NH}^{trans}	r_{NH}^{cis}	r_{CN}	α_1	α_2	α_3	$\Sigma_i\alpha_i$	τ^{trans}	τ^{cis}
				3D					
$v_{inv}=0$	1.01200	1.01501	1.37381	117.32	119.19	117.55	354.07	15.5	8.6
$v_{inv}=1$	1.01432	1.01705	1.38018	114.92	116.85	115.52	347.29	24.4	14.2
$v_{inv}=2$	1.01584	1.01829	1.38399	113.32	115.41	114.51	343.25	28.5	16.5
Tav[b]	1.01233	1.01530	1.37470	116.98	118.86	117.28	353.12	16.7	9.3
				1D					
$v_{inv}=0$	1.01138	1.01378	1.37192	118.04	119.59	117.84	355.47	16.0	8.0
$v_{inv}=1$	1.01357	1.01583	1.37809	115.79	117.35	115.60	348.73	24.5	14.1
$v_{inv}=2$	1.01487	1.01704	1.38176	114.78	116.04	114.29	344.81	28.2	16.6

[a] Bond distances in Å, valence angles in degrees. [b] Thermal average values ($T=300$ K).

TABLE 4: Experimental and Calculated Vibrational Frequencies of *trans*-*N*-Methylformamide (in cm^{-1})

mode	exp[a]	exp[b]	calc 1[c]	calc 3[d]	calc 4[e]	calc 5[f]	calc 6[g]	calc 7[h]
ν_{NH}	**3480**	3490	3867	3665	**3502**	3498		
ν_{CN}	**1201**	1207	1304	1248	**1330**	1258		
$\nu_{(Me)CN}$	**946**	951	1001	983	**1029**	1128		
ν_{inv}			328		**251**	264	**249**	260
$2\nu_{inv}$					**570**	601	**568**	601
$3\nu_{inv}$					**918**	986	**913**	980

[a] Reference 55. [b] Reference 56. [c] Calculated using the class II peptide quantum mechanical force field.[17] [d] This study: harmonic approximation. [e] This study: 3D calculations ("exact" kinetic energy). [f] This study: 3D calculations (approximate kinetic energy). [g] This study: 1D calculations ("exact" kinetic energy). [h] This study: 1D calculations (approximate kinetic energy).

with dihedral deformations. The accuracy of the separation of valence bending motions from out-of-plane motion does not seem to be as promising. Therefore, to gain insight into its limitations, three-dimensional calculations are also performed, which account explicitly for all the valence bending motion interactions (see (5)).

The results of the actual calculations are collected and compared with the experiment in Tables 1−3. As can be seen in Table 1 (the columns "calc 3" and "calc 6"), the assumption of accurate separability of pyramidalization motion from the other vibrational motions is nicely corroborated: The three and one-dimensional inversional (out-of-plane) energies coincide closely. It should be emphasized, however, that caution is required when accounting for kinematic effects: The approximate kinetic energy operator obtained in this study by disregarding the stretching intermode kinematic couplings and vibrational dependence of the inversional reduced mass does not allow for quantitative calculations (cf. "calc 4" vs "calc 5" and "calc 6" vs "calc 7"). Not surprisingly, the description of the inversional (out-of-plane) motion by means of harmonic approximation is thoroughly inadequate.

Apart from the close coincidence of the nonrigid-bender and rigid-bender inversional energies, there is also a close harmony between the corresponding effective geometries of the ground vibrational state (see the rows "calc 3" and "calc 4" in Table 2). Importantly, the calculated characteristics reasonably coincide with their counterparts derived from the microwave data under the assumption of a nonplanar molecular structure. In other words, the calculated effective geometries agree reasonably well with the experimental data, thus showing the correctness of the

TABLE 5: Inversional Molecular Geometries of *trans*-*N*-Methylformamide[a]

state	$r_{NC(Me)}$	r_{NH}	$r_{NC(O)}$	α_1	α_2	α_3	$\Sigma_i\alpha_i$	τ^{trans}	τ^{cis}
equil[b]	1.45888	1.01139	1.36323	118.52	120.55	120.93	360.0	0.0	0.0
				3D					
$v_{inv}=0$	1.45958	1.01286	1.36664	116.85	118.68	121.58	357.11	9.3	6.3
$v_{inv}=1$	1.46213	1.01450	1.37157	115.17	117.15	120.43	352.75	16.6	11.5
$v_{inv}=2$	1.46439	1.01527	1.37390	114.39	116.33	119.45	350.17	17.8	12.2
Tav[c]	1.45984	1.01300	1.36707	116.71	118.54	121.46	356.71	12.5	8.2
				1D					
$v_{inv}=0$	1.45950	1.01284	1.36660	116.86	118.70	121.61	357.17	9.3	6.3
$v_{inv}=1$	1.46193	1.01447	1.37149	115.19	117.18	120.51	352.88	16.6	11.5
$v_{inv}=2$	1.46416	1.01525	1.37385	114.40	116.37	119.55	350.32	17.8	12.2

[a] Bond distances in Å, valence angles in degrees. Experimental values:[57] $r_{NC(Me)}=1.459(6)$, $r_{NC(O)}=1.366(8)$, $\alpha_3=121.4(9)$. [b] This study, equilibrium structure. [c] Thermal average values ($T=300$ K).

TABLE 6: Experimental and Calculated Vibrational Frequencies of *cis*-*N*-Methylformamide (in cm^{-1})

mode	exp[a]	calc 1[b]	calc 3[c]	calc 4[d]	calc 5[e]	calc 6[f]	calc 7[g]
ν_{NH}	**3452**	3811	3632	**3483**	3480		
ν_{CN}	**1302**	1386	1307	**1335**	1257		
$\nu_{(Me)CN}$	**1144**	1069	1018	**1026**	1132		
ν_{inv}		−75		**259**	272	**248**	259
$2\nu_{inv}$				**564**	599	**545**	578
$3\nu_{inv}$				**869**	962	**865**	934

[a] Reference 56. [b] Calculated using the class II peptide quantum mechanical force field.[17] [c] This study: harmonic approximation. [d] This study: 3D calculations ("exact" kinetic energy). [e] This study: 3D calculations (approximate kinetic energy). [f] This study: 1D calculations ("exact" kinetic energy). [g] This study: 1D calculations (approximate kinetic energy).

profoundly nonplanar geometries predicted for higher inversional states (see Table 3).

***trans*- and *cis*-*N*-Methylformamide**. Having the N atom attached to two carbon atoms, *N*-methylformamides seem to be more suitable model systems for studying the peptide bond than formamide (interestingly enough, the OCNH configuration of the more stable *trans* isomer is adopted by the great majority of natural peptides). Unfortunately, the relevant experimental data are too scarce to allow for a detailed testing of the probed theory. Nevertheless, as can be seen in Tables 4−7, the actual calculations (the very same as in the case of formamide) prove reasonable adequacy of the semirigid-bender approach for describing the dynamics of the low-frequency out-of-plane motion and its dominant influence on the dynamical geometry parameters. As in the case of formamide, the calculations show the failure of the standard harmonic approximation to provide a reasonable description of the pyramidalization phenomena. Although the performance in describing the medium-frequency molecular motions (both stretching and bending) is poor, the adiabatic separation works reasonably for the high-frequency NH stretching motion.

***N*,*N*-Dimethylformamide**. Having substituted its peptidic hydrogen by methyl, the molecule appears to be a less suitable model system than methylformamides. Moreover, the molecular dynamics is strongly complicated by the coupled torsions of its methyl groups. Consequently, the only available (electron diffraction) geometry data[51] are insufficient for us to be able to determine the molecular geometry decisively, and adequate nonrigid-bender theoretical models have too high a dimensionality to be practical. For these reasons, only one-dimensional semirigid-bender calculations were performed. Qualitatively, as can be seen in Table 8, the results are similar to those obtained for formamide and methylformamides: Despite of planarity of the equilibrium configuration, the average geometries are significantly distorted from this configuration. On the contrary, the predicted dihedral deformations are not in quantitative agreement with their counterparts derived from the experiment. The resolution of this disharmony would require either additional experimental data or much more extensive theoretical calculations. In any case, the OCNC unit of *N*,*N*-dimethylformamide exhibits similar dynamical behavior as the OCNH unit in the remaining studied systems.

L-Alanyl-L-alanine and *N*-Benzoylphenylalanine. In principle, these two molecules can both be studied at the same level of theory as the previous models. In practice, however, these calculations would be highly impractical and certainly not extendable to larger peptides, which are of real interest. Therefore, to probe the prospects of the procedures that make calculations on large molecules feasible, we performed our calculations using the RI-MP2 and RI-CC2 *ab initio* methods and only a one-dimensional semirigid-bender dynamical model. The results of these calculations are shown in Tables 9 and 10. A brief inspection of these tables reveals fairly reasonable harmony between the calculated and experimentally determined characteristics. Importantly, the geometry characteristics calculated using the Wilson−Decius **G** matrix representation for the molecular kinetic energy operators closely agree with their "exact" counterparts, thus proving physical legitimacy of this simplifying approximation, which avoids the awkward tedium of the exact evaluation of the kinetic energy operator (see, e.g., ref 52).

TABLE 7: Inversional Molecular Geometries of *cis*-*N*-Methylformamide[a]

state	$r_{NC(Me)}$	r_{NH}	$r_{NC(O)}$	α_1	α_2	α_3	$\Sigma_i\alpha_i$	τ^{trans}	τ^{cis}
equil[b]	1.45523	1.01488	1.36688	116.24	120.28	123.48	360.0	0.0	0.0
				3D					
$\upsilon_{inv} = 0$	1.46480	1.01504	1.36989	116.95	119.78	120.55	357.28	6.5	8.4
$\upsilon_{inv} = 1$	1.46806	1.01627	1.37463	115.65	118.10	119.09	352.84	11.8	15.7
$\upsilon_{inv} = 2$	1.47045	1.01707	1.37785	114.80	117.00	118.11	349.91	12.9	17.6
Tav[c]	1.46501	1.01512	1.37019	116.87	119.68	120.45	357.00	6.8	8.8
				1D					
$\upsilon_{inv} = 0$	1.46481	1.01514	1.36979	117.07	119.47	120.65	357.19	6.7	8.7
$\upsilon_{inv} = 1$	1.46754	1.01653	1.37437	115.58	117.98	119.15	352.71	12.2	16.1
$\upsilon_{inv} = 2$	1.46952	1.01740	1.37785	114.63	117.02	118.20	349.85	13.0	18.9

[a] Bond distances in Å, valence angles in degrees. [b] This study, equilibrium structure. [c] Thermal average values ($T = 300$ K).

TABLE 8: 1D Inversional Molecular Geometries and Energies of *N*,*N*-Dimethylformamide[a]

state	r_{NC1}	r_{NC3}	r_{NC4}	α_1	α_2	α_3	$\Sigma_i\alpha_i$	τ^{trans}	τ^{cis}	E_{inv}
equil[b]	1.45484	1.45255	1.36731	117.54	121.55	120.91	360.0	0.0	180.0	
exp[c]	1.453(4)	1.453(4)	1.391(7)	113.9(5)	122.3(4)	120.8(3)	357.0	11.4(39)	16.3(45)	
$\upsilon_{inv} = 0$	1.45585	1.45375	1.36871	117.24	120.96	120.32	358.52	4.7	6.8	0.0
$\upsilon_{inv} = 1$	1.45753	1.45580	1.37120	116.67	119.98	119.37	356.02	8.6	12.9	159
$\upsilon_{inv} = 2$	1.45881	1.45737	1.37313	116.22	119.24	118.69	354.15	9.7	14.8	342
Tav[d]	1.45607	1.45402	1.36904	117.17	120.83	120.20	358.20	5.1	7.4	

[a] Bond distances in Å, valence angles in degrees, energies in cm^{-1}. [b] *Ab initio* equilibrium structure determined in this study. [c] Experimental geometry parameters (r_g bond lengths and r_α bond angles).[51] [d] Thermal average values ($T = 300$ K).

TABLE 9: 1D Inversional Molecular Geometries of L-Alanyl-L-alanine[a]

state	r_{CN}	r_{NH}	α_1	α_2	α_3	$\Sigma_i\alpha_i$	τ^{trans}	τ^{cis}	E_{inv}
equil[b]	1.362	1.016	116.7	121.9	121.4	360.0	0.8	0.5	
exp[c]	1.346	0.943	117.8	119.2	122.9	359.9	6.6	4.3	
				T_{kin}^{exact}					
$\upsilon_{inv}=0$	1.366	1.016	115.9	121.1	120.5	357.5	6.2	4.5	0.0
$\upsilon_{inv}=1$	1.370	1.018	114.5	119.7	119.1	353.3	14.8	10.9	304
$\upsilon_{inv}=2$	1.373	1.019	113.5	118.8	118.2	350.4	17.3	13.1	638
				T_{kin}^{appr}					
$\upsilon_{inv}=0$	1.366	1.016	115.9	121.1	120.5	357.5	6.4	4.7	0.0
$\upsilon_{inv}=1$	1.370	1.018	114.4	119.6	119.1	353.1	15.1	11.1	313
$\upsilon_{inv}=2$	1.374	1.019	113.3	118.5	117.9	349.7	18.5	13.5	668

[a] Bond distances in Å, valence angles in degrees. [b] This study, equilibrium structure. [c] Experimental geometry parameters.[58]

TABLE 10: 1D Inversional Molecular Geometries of *N*-Benzoylphenylalanine[a]

state	r_{CN}	r_{NH}	α_1	α_2	α_3	$\Sigma_i\alpha_i$	τ^{trans}	τ^{cis}	E_{inv}^{a}
equil[b]	1.385	1.021	116.3	117.9	119.8	354.0	22.0	6.2	
exp[c]	1.340	1.009	116.7	118.2	120.2	355.1	23.9	2.6	
				T_{kin}^{exact}					
$\upsilon_{inv}=0$	1.382	1.021	116.2	117.7	119.7	353.6	19.1	7.3	0.0
$\upsilon_{inv}=1$	1.382	1.020	116.4	117.9	119.9	354.2	16.9	7.1	343
$\upsilon_{inv}=2$	1.386	1.022	115.1	116.6	118.6	350.3	23.0	9.1	598
				T_{kin}^{appr}					
$\upsilon_{inv}=0$	1.382	1.021	116.1	117.7	119.6	353.4	19.3	7.4	0.0
$\upsilon_{inv}=1$	1.382	1.021	116.2	117.8	119.7	353.7	17.9	7.3	345
$\upsilon_{inv}=2$	1.387	1.022	114.9	116.4	118.4	349.7	23.7	9.5	628

[a] Bond distances in Å, valence angles in degrees. [b] This study, equilibrium structure. [c] Experimental geometry parameters.[59]

Conclusions

The collective "pyramidalization" vibrational distortion (removed from the vibrational dynamical problem and considered as a generalized rotation by allowing the molecular reference configuration to be a function of the out-of-plane motion coordinate) of the peptide unit OCNH in the formamide, *cis*-*N*-methylformamide, *trans*-*N*-methylformamide, *N*,*N*-dimethylformamide, L-alanyl-L-alanine, and *N*-benzoylphenylalanine molecules can be adiabatically separated from the other molecular motions. The separation allows for a physically correct description of the effective (dynamical) "ground vibrational state" molecular geometry of the OCNH unit of the studied molecules. It is therefore not unthinkable to expect that the same separation would allow for reliable estimating of the dynamical effects on the geometry of the peptide unit in larger molecular systems.

The "pyramidalization" motion of OCNH is profoundly curvilinear and anharmonic. Hence, it cannot be described properly using the concept of the standard normal coordinate. The motion is opposed by a pot-like potential with a very flat bottom, which makes OCNH fairly floppy. Because of this, the equilibrium structure of OCNH does not truly reflect its "physical" structure, which is much better represented by the vibrationally averaged structures.

The NH stretching frequency of the peptide bond of the studied model systems exhibits a high degree of the adiabatic separability from the other vibrational motions and thus seems to be a simple indicator of the presence and strengths of a peptidic NH bond.[53]

Acknowledgment. This work was a part of the research project Z40550506 and was supported by the Ministry of Education, Youth and Sports of the Czech Republic (the grant No. LC512), by the Czech Science Foundation (the grants No. 203/06/0420, 203/06/1727 and 138/81) and by the Grant Agency of the Academy of Sciences of the Czech Republic (the grant No. A400550702).

References and Notes

(1) Pauling, L.; Corey, R. B.; Branson, H. R. *Proc. Natl. Acad. Sci. U.S.A.* **1951**, *37*, 205−211.
(2) Pauling, L.; Corey, R. B. *Proc. Natl. Acad. Sci. U.S.A.* **1951**, *37*, 251−256.
(3) Ramachandran, G. N. *Biopolymers* **1968**, *6*, 1494−1496.
(4) Esposito, L.; De Simone, A.; Zagari, A.; Vitagliano, L. *J. Mol. Biol.* **2005**, *347*, 483−487.
(5) Guo, H; Karplus M. *J. Phys. Chem.* **1992**, *96*, 7273−7287.
(6) Hu, J.−S.; Bax A. *J. Am. Chem. Soc.* **1997**, *119*, 6360−6368.
(7) Mannfors, B. E.; Mirkin, N. G.; Palmo, K.; Krimm, S. *J. Phys. Chem.* **2003**, *107*, 1825−1832.
(8) Buck, M.; Karplus M. *J. Am. Chem. Soc.* **1999**, *121*, 9645−9658.
(9) Ohwada, T. *Yakugaku Zasshi* **2001**, *121*, 65−77.
(10) MacArthur, M. W.; Thornton, J. M. *J. Mol. Biol.* **1996**, *264*, 1180−1195.
(11) Kang, B. S.; Devedjiev, Y.; Derewenda, U.; Derewenda, Z. S. *J. Mol. Biol.* **1996**, *338*, 483−493.
(12) Thaimattam, R.; Jaskolski, M. J. *All. Comp.* **2004**, *362*, 12−20.
(13) Dasgupta, A. K.; Majumdar, R.; Bhattacharyya, D. *Ind. J. Biochem. Biophys.* **2004**, *41*, 233−240.
(14) Wilson, K. S.; Butterworth, S.; Dauter, Z.; Lamzin, V. S.; Walsh, M.; Wodak, S.; Pontius, J.; Richelle, J.; Vaguine, A.; Sander, C.; Hooft, R. W. W.; Vriend, G.; Thornton, J. M.; Laskowski, R. A.; MacArthur, M. W.; Dodson, E. J.; Murshudov, G.; Oldfield, T. J.; Kaptein, R.; Rullman, J. A. C. *J. Mol. Biol.* **1998**, *276*, 417−436.
(15) Reif, B.; Hennig, M.; Griesinger, C. *Science* **1997**, *276*, 1230−1233.
(16) Daragan, V. A.; Mayo, K. H. *Prog. Nucl. Magn. Reson. Spectrosc.* **1997**, *31*, 63−105.
(17) Maple, J. R.; Hwang, M.-J.; Jalkanen, K. J.; Stockfisch, T. P.; Hagler, A. T. *J. Comput. Chem.* **1998**, *19*, 430−458.
(18) Bludský, O.; Šponer, J.; Leszczynski, J.; Špirko, V.; Hobza, P. *J. Chem. Phys.* **1996**, 11042−11050.
(19) Brown, R. D.; Godfrey, P. D.; Kleibömer, B. *J. Mol. Spectrosc.* **1987**, *124*, 34−45.
(20) Bunker, P. R.; Landsberg, B. M. *J. Mol. Spectrosc.* **1977**, *67*, 374−385.
(21) Brown, R. D.; Godfrey, P. D.; Kleibömer, B. *J. Mol. Spectrosc.* **1985**, *114*, 257−273.
(22) Brown, R. D.; Godfrey, P. D.; Kleibömer, B. *J. Mol. Spectrosc.* **1987**, *124*, 21−33.
(23) Hoy, A. R.; Bunker, P. R. *J. Mol. Spectrosc.* **1974**, *52*, 439−456.
(24) Špirko, V. *J. Mol. Spectrosc.* **1983**, *101*, 30−47.
(25) Špirko, V.; Kraemer, W. P. *J. Mol. Spectrosc.* **2000**, *199*, 236−244.
(26) Špirko, V.; Čejchan, A.; Lutchyn, R.; Leszczynski, J. *Chem. Phys. Lett.* **2002**, 319−326.
(27) Frisch, M. J.; Trucks, G. W.; Schlegel, H. B.; Scuseria, G. E.; Robb, M. A.; Cheeseman, J. R.; Montgomery, J. A., Jr.; Vreven, T.; Kudin, K. N.; Burant, J. C.; Millam, J. M.; Iyengar, S. S.; Tomasi, J.; Barone, V.; Mennucci, B.; Cossi, M.; Scalmani, G.; Rega, N.; Petersson, G. A.; Nakatsuji, H.; Hada, M.; Ehara, M.; Toyota, K.; Fukuda, R.; Hasegawa, J.; Ishida, M.; Nakajima, T.; Honda, Y.; Kitao, O.; Nakai, H.; Klene, M.; Li, X.; Knox, J. E.; Hratchian, H. P.; Cross, J. B.; Bakken, V.; Adamo, C.; Jaramillo, J.; Gomperts, R.; Stratmann, R. E.; Yazyev, O.; Austin, A. J.; Cammi, R.; Pomelli, C.; Ochterski, J. W.; Ayala, P. Y.; Morokuma, K.; Voth, G. A.; Salvador, P.; Dannenberg, J. J.; Zakrzewski, V. G.; Dapprich, S.; Daniels, A. D.; Strain, M. C.; Farkas, O.; Malick, D. K.; Rabuck, A. D.; Raghavachari, K.; Foresman, J. B.; Ortiz, J. V.; Cui, Q.; Baboul, A. G.; Clifford, S.; Cioslowski, J.; i Stefanov, B. B.; Liu, G.; Liashenko, A.; Piskorz, P.; Komaromi, I.; Martin, R. L.; Fox, D. J.; Keith, T.; Al−Laham, M. A.; Peng, C. Y.; Nanayakkara, A.; Challacombe, M.; Gill, P. M. W.; Johnson, B.; Chen, W.; Wong, M. W.; Gonzalez, C.; Pople, J. A. *Gaussian*; Gaussian, Inc.: Wallingford, CT, 2004.
(28) (a) Moller, C.; Plesset, M. S. *Phys. Rev.* **1934**, *46*, 618−622. (b) Head-Gordon, M.; Pople, J. A.; Frisch, M. J. *Chem. Phys. Lett.* **1988**, *153*, 503−506. (c) Frisch, M. J.; Head-Gordon, M.; Pople, J. A. *Chem. Phys. Lett.* **1990**, *166*, 275−280. (d) Frisch, M. J.; Head-Gordon, M.; Pople, J. A. *Chem. Phys. Lett.* **1990**, *166*, 281−289. (e) Head-Gordon, M.; Head-Gordon, T. *Chem. Phys. Lett.* **1994**, *220*, 122−128. (f) Saebo, S.; Almlof. *Chem. Phys. Lett.* **1989**, *154*, 83−89.
(29) (a) Woon, D. E.; Dunning, T. H., Jr. *J. Chem. Phys.* **1993**, *98*, 1358−1371. (b) Kendall, R. A.; Dunning, T. H., Jr.; Harrison, R. J. *J. Chem. Phys.* **1992**, *96*, 6796−6806.
(30) Allen, F. H. *Acta Crystallogr. B* **2002**, 58, 380−388.

(31) Tokuma, Y; Ashida, T.; Kakudo, M. *Acta Crystallogr. B* **1969**, *25*, 1367−1373.
(32) Potrzebowski, M. J.; Tekely, P.; Baszczyk, J.; Wieczorek, M. W. *J. Pept. Res.* **2000**, *56*, 185−194. (b) Kendall, R. A.; Dunning, T. H., Jr.; Harrison, R. J. *J. Chem. Phys.* **1992**, *96*, 6796−6806.
(33) (a) Weigend, F.; Häser, M. *Theor. Chem. Acc.* **1997**, *97*, 331−340. (b) Feyereisen, M.; Fitzgerald, G.; Komornicki, A. *Chem. Phys. Lett.* **1993**, *208*, 359−363. (c) Vahtras, O.; Almlof, J.; Feyereisen, M. W. *Chem. Phys. Lett.* **1993**, *213*, 514−518. (d) Haase, F.; Ahlrichs, R. *J. Comput. Chem.* **1993**, *14*, 907−912.
(34) (a) Becke, A. D. *Phys. Rev. A* **1988**, *38*, 3098−3100. (b) Lee, C.; Yang, W.; Parr, R. G. *Phys. Rev. B* **1988**, *37*, 785−789. (c) Vosko, S. H.; Wilk, L.; Nusair, M. *Can. J. Phys.* **1980**, *58*, 1200−1211. (d) Becke, A. D. *J. Chem. Phys.* **1993**, *98*, 5648−5652.
(35) Hehre, W. J.; Radom, L.; Schleyer, P. v. R.; Pople, J. A. *Ab initio molecular orbital theory*; Wiley−Interscience: New York, 1986.
(36) (a) Pople, J. A.; Krishnan, R.; Schlegel, H. B.; Binkley, J. S. *Int. J. Quantum Chem.* **1978**, *14*, 545−560. (b) Bartlett, R. J.; Purvis, G. D. *Int. J. Quantum Chem.* **1978**, *14*, 561−581. (c) Čížek, J. *Adv. Chem. Phys.* **1969**, *14*, 35−89. (d) Purvis, G. D.; Bartlett, R. J. *J. Chem. Phys.* **1982**, *76*, 1910−1918. (e) Scuseria, G. E.; Janssen, C. L.; Schaefer, H. F., III. *J. Chem. Phys.* **1988**, *89*, 7382−7387. (f) Scuseria, G. E.; Schaefer, H. F., III. *J. Chem. Phys.* **1989**, *90*, 3700−3703.
(37) (a) Christiansen, O.; Koch, H.; Jörgensen, P. *Chem. Phys. Lett.* **1995**, *243*, 409−418. (b) Hättig, C.; Weigend, F. *J. Chem. Phys.* **2000**, *113*, 5154−5161.
(38) Ahlrichs, R.; Bär, M.; Häser, M.; Horn, H.; Kölmel, C. *Chem. Phys. Lett.* **1989**, *162*, 165−169.
(39) Weigend, F.; Köhn, A.; Hättig, C. *J. Chem. Phys.* **2002**, *116*, 3175−3183.
(40) Hougen, J. T.; Bunker, P. R.; Johns, J. W. C. *J. Mol. Spectrosc.* **1970**, *34*, 136−172.
(41) Kuchitsu, K. *J. Chem. Phys.* **1968**, *49*, 4456−4462.
(42) Kurland, R. J.; Wilson, E. B. *J. Chem. Phys.* **1957**, *27*, 585−590.
(43) Costain, C. C.; Dowling, J. M. *J. Chem. Phys.* **1960**, *32*, 158−165.
(44) Hirota, E.; Sugisaki, C. J.; Nielsen, C. J.; Sörensen, G. O. *J. Mol. Spectrosc.* **1974**, *49*, 251−267.
(45) Evans, J. C. *J. Chem. Phys.* **1954**, *22*, 1228−1234.
(46) King, S. T. *J. Phys. Chem.* **1971**, *75*, 405−410.
(47) Rubalcava, H. Dissertation, Caltech, 1956.
(48) Hansen, E. L.; Larsen, N. W.; Nicolaisen, F. M. *Chem. Phys. Lett.* **1980**, *69*, 327−331.
(49) Carlsen, N. R.; Radom, L.; Riggs, N. V.; Rodwell, W. R. *J. Am. Chem. Soc.* **1979**, *101*, 2233−2234.
(50) Fogarasi, G.; Szalay, P. G. *J. Phys. Chem. A* **1997**, *101*, 1400−1408.
(51) Schultz, G.; Hargittai, I. *J. Phys. Chem.* **1993**, *97*, 4966−4969.
(52) Čejchan, A.; Špirko, V. *J. Mol. Spectrosc.* **2003**, *217*, 142−145.
(53) Mirkin, N. M.; Krimm, S. *J. Phys. Chem. A* **2004**, *108*, 5438−5448.
(54) Kitano, M; Kuchitsu, K. *Bull. Chem. Soc. Jpn.* **1974**, *47*, 67−72.
(55) Jones, R. L. *J. Mol. Spectrosc.* **1958**, *2*, 581−586.
(56) Ataka, S.; Takeuchi, H.; Tasumi, M. *J. Mol. Struct.* **1984**, *113*, 147−160.
(57) Kitano, M.; Kuchitsu, K. *Bull. Chem. Soc. Jpn.* **1974**, *47*, 631−634.
(58) Fletterick, R. J.; Tsai, C. C.; Hughes, R. E. *J. Phys. Chem.* **1971**, *75*, 918−922.
(59) Kazmierski, S.; Olejniczak, S.; Potrzebowski, M. J. *Solid State Nucl. Magn.* **2000**, 131−139.